1860–1871 *Nucleic Acids Research, 2017, Vol. 45, No. 4* *Published online 13 December 2016*
doi: 10.1093/nar/gkw1210

RMI1 and TOP3α limit meiotic CO formation through their C-terminal domains

Mathilde Séguéla-Arnaud, Sandrine Choinard, Cécile Larchevêque, Chloé Girard, Nicole Froger, Wayne Crismani and Raphael Mercier*

Institut Jean-Pierre Bourgin, INRA, AgroParisTech, CNRS, Université Paris-Saclay, RD10, 78000 Versailles, France

Received May 17, 2016; Revised November 17, 2016; Editorial Decision November 18, 2016; Accepted November 23, 2016

ABSTRACT

At meiosis, hundreds of programmed DNA double-strand breaks (DSBs) form and are repaired by homologous recombination. From this large number of DSBs, only a subset yields crossovers (COs), with a minimum of one CO per chromosome pair. All DSBs must be repaired and every recombination intermediate must be resolved to avoid subsequent entanglement and chromosome breakage. The conserved BLM-TOP3α-RMI1 (BTR) complex acts on early and late meiotic recombination intermediates to both limit CO outcome and promote chromosome integrity. In *Arabidopsis*, the BLM homologues RECQ4A and RECQ4B act redundantly to prevent meiotic extra COs, but recombination intermediates are fully resolved in their absence. In contrast, TOP3α is needed for both processes. Here we show through the characterization of specific mutants that RMI1 is a major anti-CO factor, in addition to being essential to prevent chromosome breakage and entanglement. Further, our findings suggest a specific role of the C-terminal domains of RMI1 and TOP3α, that respectively contain an Oligo Binding domain (OB2) and ZINC finger motifs, in preventing extra-CO. We propose that these domains of TOP3α and RMI1 define a sub-domain of the BTR complex which is dispensable for the resolution of recombination intermediates but crucial to limit extra-COs.

INTRODUCTION

Homologous recombination (HR) is a highly conserved pathway for the repair of DNA double strand breaks (DSBs) and is essential at meiosis. At the onset of this specialized cell division, a large number of DSBs are formed, repaired by HR, and a subset matures as crossovers (COs). These reciprocal exchanges of genetic material between homologous chromosomes, in addition to generating novel combinations of alleles, ensure their accurate segregation at meiosis I. The remaining DSBs that are not designated as COs are repaired as local and non-reciprocal exchange of genetic material (non-crossovers, NCOs) or using the sister chromatid as a template, to avoid DNA fragmentation and safeguard chromosome integrity. Meiotic HR is a tightly regulated process that brings into play multiple processing enzymes (1).

Meiotic HR is initiated by the programmed formation of DSBs by the SPO11 transesterase. DSBs are resected to generate 3′ single-stranded DNA overhangs which invade the intact homologous chromosome to initiate the repair. DNA strand invasion results in the formation of structures called displacement loops (D-loops) or joint molecules (JMs) that can be subsequently processed as COs or NCOs by different pathways. In most eukaryotes, including plants, budding yeast and mammals, JM maturation as COs is mainly under the control of the ZMM-dependent pathway (for Zip1-4, Msh4/5 and Mer3) (1–3). This group of proteins stabilizes nascent JMs and promotes the formation of double Holliday junctions (dHJs) (4). The MutL homologs 1 and 3 (MLH1 and MLH3) resolve these structures as interfering COs (i.e. occurring more widely and evenly spaced than would occur by chance), also referred to as class I COs (1,5). A second minor pathway, producing non-interfering COs (class II CO), exists and relies on structure-specific endonucleases including MUS81 (6–8). Nevertheless, these two CO pathways together process only a subset of recombination intermediates, the rest being processed as NCOs. In many species, such as *Arabidopsis* and mouse, it is estimated that COs represent the repair outcome of only 5 to 10% of DSBs (9,10).

The highly conserved BTR complex (BLOOM-TOP3α-RMI1-RMI2 in human and Sgs1-Top3-Rmi1 in budding yeast) is a major NCO promoting factor and its different members play several roles at meiosis both as a complex or independently (5,11–16). The first biochemical activity

*To whom correspondence should be addressed. Tel: +33 1 30 83 39 89; Fax: +33 1 30 83 33 19; Email: raphael.mercier@versailles.inra.fr
Present addresses:
Chloé Girard, Department of Developmental Biology, Stanford University School of Medicine, Stanford, CA, USA.
Wayne Crismani, Genome Stability Unit, St Vincent's Institute of Medical Research, Fitzroy, Victoria 3065, Australia.

described for the BTR complex was its unique ability to dissolve dHJs, a process that yields exclusively NCOs (17). During this reaction, the two junctions of the dHJ are migrated towards each other by the BLM/Sgs1 helicase. The structure generated, called hemicatenane, is then removed by TOP3α, and its co-factor RMI1 (18–20). The second biochemical activity described for the complex is the unwinding of D-loops that exclusively promotes the formation of NCOs through the synthesis-dependent strand annealing pathway (SDSA) (21–23). The invading strand is dissociated from the homologous chromosome after DNA synthesis and then anneals to the second end of the original DSB, resulting in the local and non-reciprocal exchange of genetic material characteristic of an NCO. Recent studies in budding yeast demonstrated that the D-loop unwinding activity, previously thought to be performed by the Sgs1 helicase alone, requires the three members of the complex (12,13,23). Further, it has been shown that Top3 and Rmi1 resolve late meiotic recombination intermediates and thus remove chromosome entanglements, independently of Sgs1 (12,13). In *Arabidopsis*, the three members of the complex are conserved and interact *in vivo*; *TOP3α* and *RMI1* are represented by single copy genes while BLOOM has two redundant homologues, RECQ4A and RECQ4B (hereafter called RECQ4A/B for simplicity) (14–16,24). The defects observed in the *Arabidopsis* BTR mutants are consistent with the dual function of the complex (Table 1): (i) TOP3α and RMI, but not RECQ4A/B, are essential for disentangling meiotic chromosomes and ensure their proper separation. (ii) Knockouts of *RECQ4A/B* and the *top3α-R640X* mutant have elevated CO frequency, without chromosome entanglement or fragmentation defects, establishing an anti-CO function for RECQ4A/B and TOP3α (16).

In this study, pursuing the identification of anti-CO activities through a genetic screen, we show that RMI1 is a major meiotic anti-CO factor in plants like its BTR co-members RECQ4A/B and TOP3α (16). The RMI1 protein was previously shown to be essential for ensuring complete resolution of meiotic recombination intermediates (14,15). We thus show that, like its partner TOP3α, RMI1 has a dual function at meiosis in limiting CO and in promoting recombination intermediates resolution, and that these functions can be uncoupled by specific mutations. Moreover, by the characterization of several *rmi1* and *top3α* alleles, we delineate the different domains of RMI1 and TOP3α proteins involved in the anti-CO function, but not essential for the repair of DSBs. We propose that the OB2 fold domain of RMI1 and the Zn-finger containing C-terminal domain of TOP3α together could form a sub-domain within the BTR complex that is required to limit CO formation at meiosis.

MATERIALS AND METHODS

Genetic resources

The lines used in this study were: *hei10-2* (N514624) (9), *fancm-1* (25), *msh4* (cshl_GT14269) (26), *msh5-2* (N526553) (27), *mus81-2* (N607515) (6), *recq4a-4* (N419423) (24), *recq4b-2* (N511130) (24), *rmi1-1* = *blap75-2* (N593589) (14,15), *rmi1-2* (N594387) (14), *rmi1-4* (N554062) (14), *rmi1-5* (N505449) (14), *rmi1-6* (N591373), *shoc1-1* (N557589) (28), *top3α-2* (N445612) (15), *top3α-R640X* (16). Tetrad analysis lines were: I2ab (FTL1506/FTL1524/FTL965/*qrt1-2*), I1bc (FTL567/FTL1262/FTL992/ *qrt1-2*) from G. Copenhaver (29). Suppressors *shoc1(S)155*, *msh4(S)48, msh4(S)146* and *hei10(S)389* were sequenced using Illumina technology (The Genome Analysis Centre, UK). Mutations were identified through the MutDetect pipeline (30). The causal mutations were C to T substitutions at positions TAIR10 (Col-0 assembly) chr5: 25441195 for *shoc1(S)155*, Ler assembly chr5: 25009361 for *msh4(s)48,* TAIR10 chr5: 25575525 for *hei10(S)389*, and G to A substitution at position Ler assembly chr5: 25147639 for *msh4(s)146*. Primers used to genotype the different T-DNA insertions and point mutations are supplied in Supplementary Table S1.

Cytology technics

Meiotic chromosome spreads have been performed as described previously (31). Immunolocalizations of MLH1 were performed as described in (32). Observations were made using a ZEISS AxioObserver microscope.

FTL analysis

For each FTL experiment, all genotypes including wild-type controls, were siblings segregating for the tested mutations. Tetrad slides were prepared as in (29) and counting was performed through an automated detection of tetrads using a pipeline developed on the Metafer Slide Scanning Platform (http://www.metasystems-international.com/metafer). For each tetrad, attribution to a specific class (A to L) was confirmed by hand (29). Genetic sizes of each interval was calculated using the Perkins equation (33): $D = 100$ x (tetratype frequency + 6 × non-parental-ditype frequency)/2 in cM. (see http://www.molbio.uoregon.edu/~fstahl for details). Fold increase was calculated by adding the genetic size of all considered intervals in the mutant, divided by the sum of the genetic size of the same intervals in the wild type.

Interference ratio was calculated as in (29), with pooled data from all the experiments containing the relevant genotypes. For two adjacent intervals I1 and I2, two populations of tetrads are considered: those with at least one CO in I2 and those without any CO in I2. The genetic size of I1 is then calculated for these two populations using the Perkins equation (above), namely D_1 (I1 with CO in I2) and D_2 (I1 without a CO in I2). The IR is thus defined as $IR = D_1/D_2$. If the genetic size of I1 is lowered by the presence of a CO in I2, $IR < 1$ and interference is detected. If not, IR is close to 1 and no interference is detected. A Z-test is performed to test the null hypothesis (H_0: $D_1 = D_2$.). The average of the two reciprocal IRs is shown on the graphs.

Yeast two hybrid

The $RECQ4A^{1\text{-}400}$, TOP3α and RMI1 open reading frames were amplified from *Arabidopsis* cDNA clones (Columbia ecotype) using specific primers flanked by the AttB1 and

Table 1. Summary of somatic and meiotic defects observed in single or multiple *btr* mutants in *Arabidopsis*

	nature of mutation	somatic	meiotic completion/catastrophe	restored CO in *zmm*
rmi1-1	likely null	ok	catastrophe	nd
rmi1-2	upstream OB2	ok	completion	yes
rmi1-G592X	within OB2	ok	completion	yes
rmi1-4	upstream OB2	ok	completion	yes
rmi1-5	upstream OB2	ok	completion	yes
rmi1-6	within OB2	ok	completion	yes
rmi1-G554R	within OB2 loop	ok	completion	yes
top3α-1	likely null	lethal	nd	nd
top3α-2	leaky	stunted growth	catastrophe	nd
top3α-R640X	STOP upstream the 4 Zn fingers	ok	completion	yes
top3α-R840	Splicing within 3rd Zn fingers	ok	completion	yes
top3α-R188C	AA change within domain IV	ok	completion	yes
recq4ab	likely null	ok	completion	yes
top3α-R640 recq4ab	-	ok	catastrophe	nd
rmi1-G592X recqab	-	ok	catastrophe	nd
top3α-R rmi1-G592x	-	stunted growth	catastrophe	nd

AttB2 sites (Supplementary Table S1), cloned into Gateway vector pDONR207 using BP recombination (Invitrogen), and sequenced. For the RMI1ΔOB1 construct, splicing of OB1 was obtained by overhang extension, using the RMI1delOB1for and RMI1delOB1rev primers (Supplementary Table S1). The RMI1ΔOB2 was amplified using the RMI1for GTW and RMI1delOB2revGTW primers (Supplementary Table S1). The TOP3α-R640X construct was obtained as described in (34) using the TOP3αmutfor and TOP3αmutrev primers (Supplementary Table S1). Expression vectors were obtained after LR recombination (Invitrogen) between these entry vectors and destination vectors (pGADT7-GW and pGBKT7-GW). Yeast two-hybrid interactions were tested using RECQ4A-Nterm, TOP3α, RMI1 and truncated versions of TOP3α or RMI1 as bait (pGADT7-GW) or as prey (pGBKT7-GW) by mating with the AH109 and Y187 yeast strains (Matchmaker™ GAL4 Two-Hybrid System 3. Clontech).

RESULTS AND DISCUSSION

zmm suppressor screen identified RMI1 as an anti-CO factor

In order to identify factors that limit COs, we designed a genetic screen in *Arabidopsis*, as described previously (16,25,30,35). Using fruit length as a proxy for the level of CO formation, we screened for suppressors of CO-deficient mutants (the *zmm* mutants; *zip4*, *shoc1 (AtZip2)*, *hei10*, *msh4* and *msh5*). Mutation of an anti-CO gene would restore the level of CO formation and therefore correct chromosome segregation and fertility of the plants. The screen led to the identification of several complementation groups and three different anti-CO pathways were previously described: (i) a pathway depending on the *FANCM* helicase and its co-factors *MHF1* and *MHF2* (25,30), (ii) the BTR pathway with *RECQ4* and *TOP3α* (16) and (iii) the *FIDGETIN-like1* pathway (35). This study consists in the characterization of a mutation (*shoc1(S)155*) that restored the fertility of *shoc1/zip2*. Meiotic chromosome spreads showed that bivalent formation was fully restored in *shoc1(S)155* compared to *shoc1-1* (Figure 1A and B), suggesting a high level of crossover restoration. Whole genome sequencing of this suppressor revealed a candidate mutation in the gene encoding the RecQ4-Mediated Instability 1 (*RMI1*) homolog (At5g63540). The identified mutation affected the splice acceptor site of the seventh intron leading to altered RMI1 coding sequence from Gly^{592}. Hence, the *shoc1(S)155* suppressor is named hereafter *shoc1 rmi1-G592X* (Figure 2 and Supplementary Figure S1). F1 plants from the complementation test between *shoc1 rmi1-G592X* and *shoc1 rmi1-1* were fertile and showed restored bivalent formation at metaphase I (Figure 1A), demonstrating that the *rmi1-G592X* mutation was the causal mutation in *shoc1(S)155*. Further, we showed that the *rmi1-G592X* mutation was able to restore bivalent formation in *msh5-2* (Figure 1A and B). We identified a suppressor of *msh4* also carrying a mutation in *RMI1* leading to $Gly^{554} \rightarrow$Arg amino acid change (hereafter *rmi1-G554R*, Figure 2A), that was associated with partial restoration of bivalent formation at metaphase I (Figure 1A and B). This shows that mutations in *RMI1* can restore CO formation in at least three different *zmm* mutants, *msh4, msh5* and *shoc1/Atzip2*, establishing an anti-CO activity to RMI1.

Two studies previously described null *Arabidopsis rmi1* mutants as sterile because of meiotic catastrophe: metaphase I bivalents have aberrant shapes, massive chromosome fragmentation and chromatin bridges are

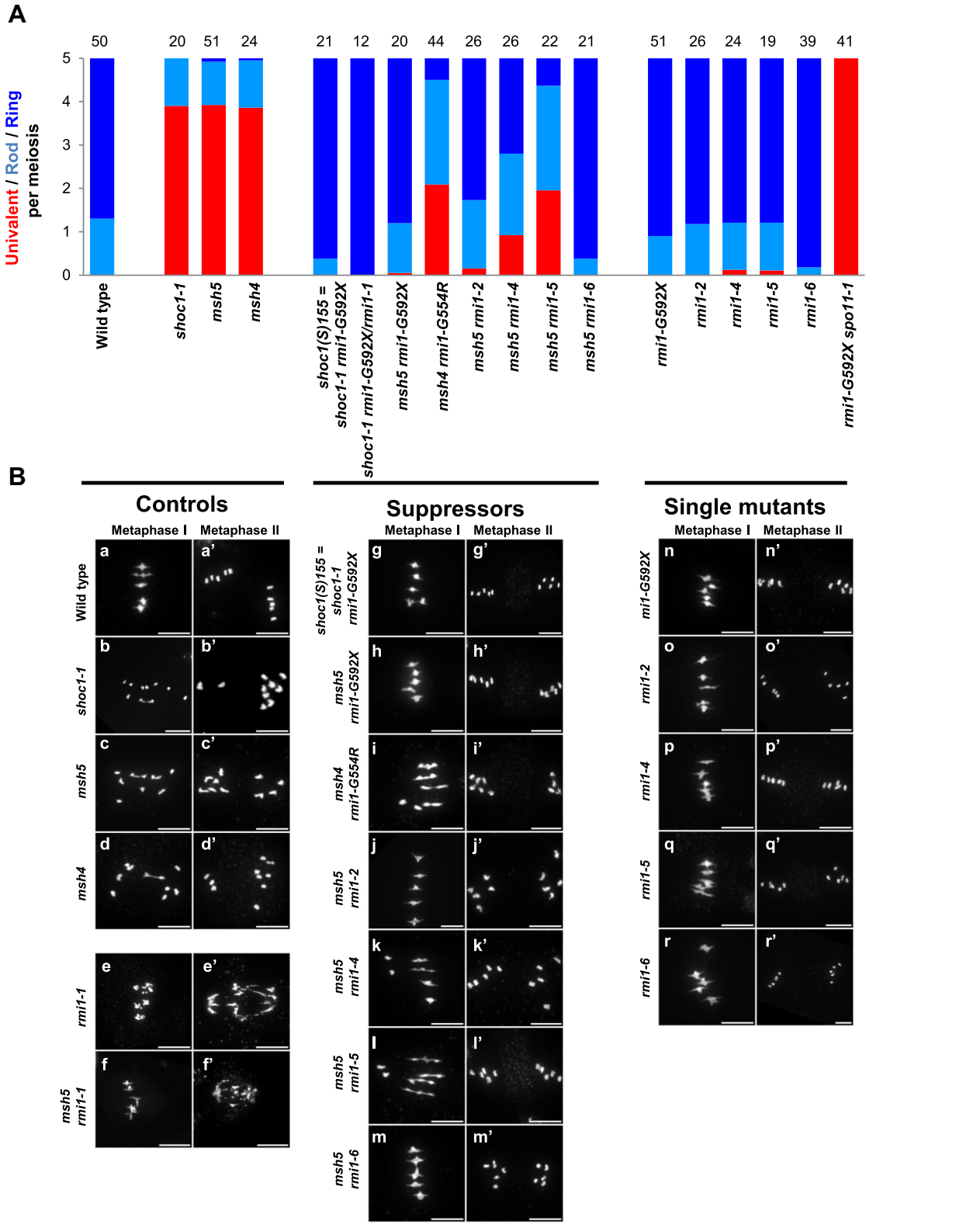

Figure 1. Separation of function mutations in RMI1 restore bivalent formation in *zmm* mutants. (**A**) Average number of bivalents per male meiocyte. Light blue bars represent rod bivalents, which have a rod shape with enlarged ends, indicating that one arm has at least one CO, whereas the other arm has no CO. Dark blue bars indicate ring bivalents, which have a lozenge shape, indicating that they have at least one CO on both arms. Red bars indicate pairs of univalents. The number of cells analyzed is indicated above each bar. (**B**) Chromosome spreads at metaphase I and metaphase II. Ring bivalents (marked as 'a' in B), rod bivalents (marked as 'b' in B), and univalents (marked as 'u' in B) are indicated (scale bars, 10 μM). For *rmi1-1* and *msh5 rmi1-1,* images of anaphase I are displayed as meiosis does not proceed further in these genotypes.

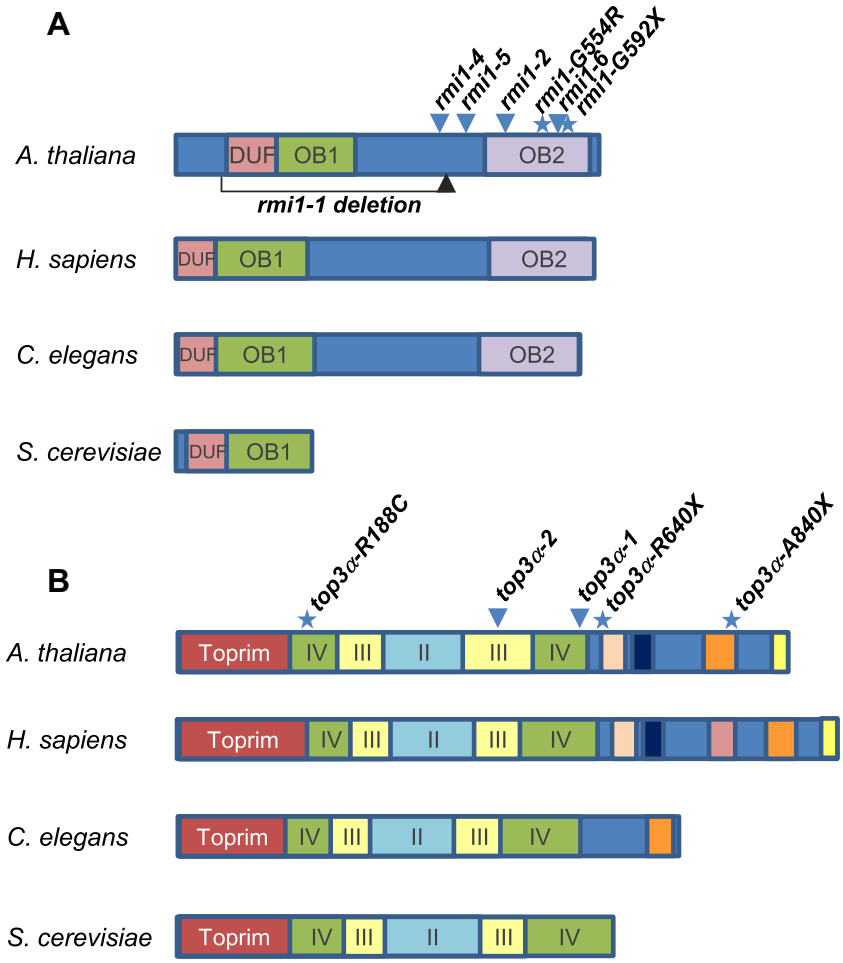

Figure 2. Domain organization of RMI1 and TOP3α proteins in representative eukaryotic species. (**A**) Schematic representation of RMI1 proteins in representative eukaryotic species. In most species, RMI1 protein contains three conserved domains: a domain of unknown function DUF1767 and two Oligo binding (OB)-fold domains. The second OB-fold domain 2 is not conserved in the yeast lineage. Positions of the mutations described in *Arabidopsis* are indicated. Triangles show the T-DNA insertion sites and point mutations are indicated with a star. The corresponding protein alignment is shown in Supplemental Figure S1. (**B**) Domain organization of TOP3α/Top3 proteins in representative eukaryotic species. Positions and nomenclature of the different domains are based on the human protein architecture described by Bocquet *et al.* (44). The Toprim domain, the gate domain (II), the catalytic 5Y cap (III) and the noncatalytic CAP domain (IV) are conserved in all species. Aside from the yeast lineage, TOP3α proteins contain from one up to five zinc finger domains. Positions of the mutations described in *Arabidopsis* are indicated as in (A). The corresponding protein alignment is shown in Supplemental Figure S1.

observed at anaphase I and meiocytes do not progress into meiosis II (14,15) (*rmi1-1* on Figure 1B). This phenotype sharply contrasts with the phenotype of *rmi1-G592X, rmi1-G592X shoc1, rmi1-G592X msh5* and *rmi1-G554R msh4* in which no chromosome fragmentation or bridges were observed at anaphase I (Figure 1B) and meiosis proceeded normally. This suggests that in null *rmi1* mutants either some recombination intermediates failed to be resolved or some unresolvable structures are formed, while all intermediates are resolved in presence of RMI1-G592X or RMI1-G554R.

Taken together, these results show that RMI1 has an anti-CO activity that can be uncoupled from its essential function in ensuring complete resolution of recombination intermediates. Two hypotheses can explain the difference of phenotype between the null *rmi1* mutants and our novel alleles. First, RMI1 might be involved in two distinct biochemical activities (i.e. processing different substrates), with the *rmi1-G592X* and *rmi1-G554R* mutations affecting specifically the activity that prevents the formation of extra-COs. Alternatively, RMI1 might have a single biochemical activity, with *rmi1-G592X* and *rmi1-G554R* being partial loss-of-function mutations that reduce this activity to a level that is still able to resolve entanglements in recombination intermediates but not to prevent extra-COs.

RMI1 is an important anti-CO factor

In order to quantify the RMI1 anti-CO function, we measured meiotic recombination in the *rmi1-G592X* mutant by tetrad analysis in a series of intervals defined by fluorescent markers expressed in pollen grains (fluorescent-tagged lines—FTLs) (29) (Figure 3A). In comparison to wild type, we observed a large increase of genetic distances on four intervals tested, with an average increase of 300% (Figure 3B). This establishes RMI1 as one of the strongest anti-CO

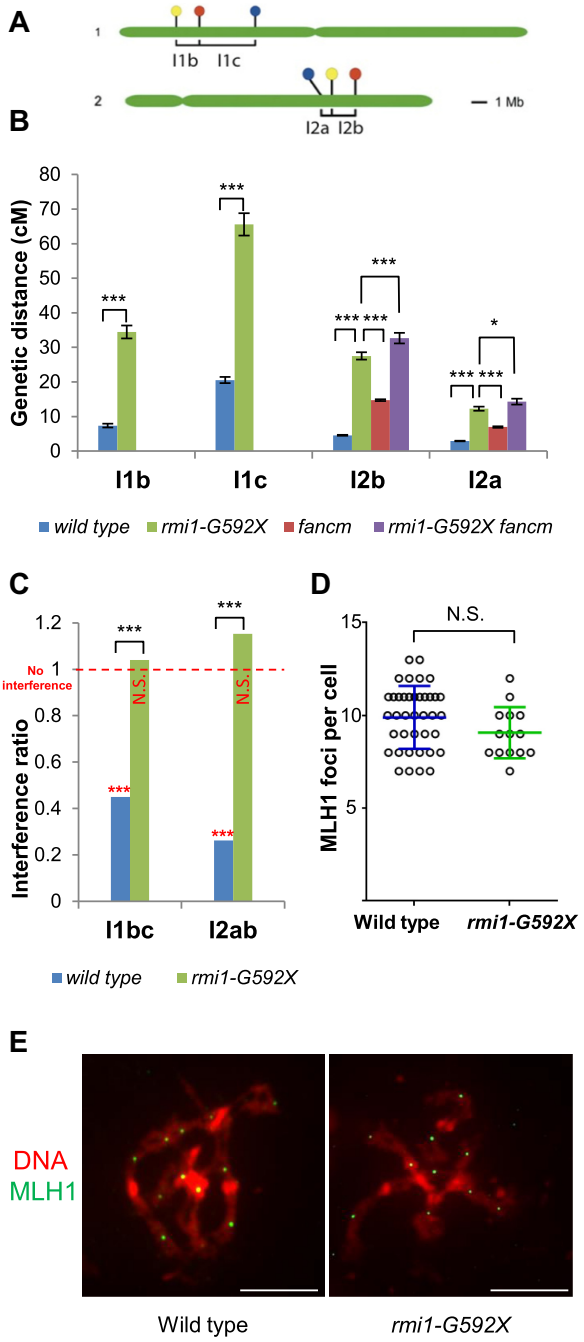

Figure 3. RMI1 limits meiotic recombination in parallel of FANCM. (**A**) Chromosomal position of the markers in the fluorescent tagged lines used in this study (I1bc and I2ab intervals). Fluorescent transgene insertion sites are indicated by a red (DsRed2), yellow (eYFP) or cyan (eCFP) circles (29). (**B**) Genetic distances measured by using fluorescent-tagged lines. The result of the test of identical recombination between genotypes is shown (*$P < 0.5$, ***$P < 0.001$). Raw data are shown in Supplementary Table S2. (**C**) Mean interference ratio (IR). The tetrad data set was used to analyze the effect of having COs in one interval on the genetic distance of the adjacent interval (interference ratio, IR). IR is close to 0 when interference is positive and IR = 1 when interference is absent (red line). The result of the test of absence of interference is shown in red (***$P < 0.001$, NS = $P > 0.05$). The result of the test of identical interference between genotypes is shown in black (***$P < 0.001$). (**D**) MLH1 foci number per cell at diakinesis. Error bars represent the mean ± standard deviation. (**E**) MLH1 immunolocalization at diakinesis (green). DNA is stained with DAPI (red) (scale bars, 10 μM).

factors described to date. RMI1, TOP3α and RECQ4A/B belong to the same protein complex (16), suggesting that they may act together to limit extra-COs (see below). On the chromosome 2 intervals (I2ab, Figure 3B), the *rmi1-G592X* led to an increase of 430%, almost as high as the *recq4ab* mutation (540% (16)) and much stronger than the effect observed in *top3α-R640X* mutants (up to 150% (16)). The increase in recombination in *rmi1-G592X* being almost as high as in *recq4ab* suggests that RMI1 is equally important as the helicase RECQ4A/B to mediate the major anti-CO activity of the BTR complex. We observed a lesser effect of *top3α-R640X* mutation on CO increase, meaning either that TOP3α is partially dispensable, or that *top3α-R640X* has kept some anti-CO activity, as previously suggested (16).

RMI1 limits class II COs and acts in parallel of FANCM

Next we asked if, like all the anti-CO factors identified so far in *Arabidopsis*, *RMI1* limits class II CO. First, we observed that interference was undetectable in *rmi1-G592X* (Figure 3C), as opposed to wild-type where interference is strong in all pairs of intervals tested. Second, immunolabeling of MLH1, which specifically the marks sites of class I CO, did not reveal any increase in foci number in *rmi1-G592X* compared to wild type (Figure 3D and E). This suggests an increase in class II COs in *rmi1-G592X*. To test if the extra COs in *rmi1-G592X* depend on the class II factor MUS81 for their formation, we aimed to combine the *rmi1-G592X* and *mus81* mutations. Among 480 plants of a population segregating for the two mutations, we did not isolate any *rmi1-G592X mus81-1* double mutants (30 expected, $P < 10^{-7}$). Further, no double mutant was isolated among 96 plants of the progeny of a plant homozygous for the *rmi1-G592X* mutation and heterozygous for the *mus81-1* mutation (24 expected, $P < 10^{-7}$), suggesting that the *rmi1-G592X mus81* double mutant is unviable. This parallels the combination of *recq4a* and *mus81* mutations that was previously shown to result in synthetic lethality and the *top3α-R640X mus81* double mutant that shows growth defects (16,36). This further supports the essential role of the BTR complex in somatic DNA repair in *Arabidopsis* (15,24). Similarly, yeast high-throughput analyses have also identified synthetic lethal interactions between *top3* or *rmi1* and *mus81* (37,38). We previously showed that *MUS81* becomes essential for full resolution of JMs at meiosis in the *top3α-R640X Arabidopsis* mutant. It is therefore possible that MUS81 also becomes essential at meiosis in the *recq4ab* and the *rmi1-G592X* mutants but the lethality of *rmi1-G592X mus81* and *recq4ab mus81* prevented us to directly test it. However, data from budding yeast, establishing that MUS81 resolves meiotic JMs in *sgs1*, *top3* and *rmi* mutants, support this possibility (5,11–13).

Finally to test if *FANCM* and *RMI1* act in the same or distinct pathways to limit CO, we generated the *rmi1-G592X fancm-1* double mutant. Meiotic progression was normal in this mutant and we measured meiotic recombination by fluorescent tetrad analysis (Figure 3B). In comparison to wild type, we observed an increase of 190% in meiotic recombination in *fancm-1*, of 430% in *rmi1-G592X* and 530% in the double *rmi1-G592X fancm-1* mutant which is higher that both single mutants (Figure 3B). Therefore, the effect of the

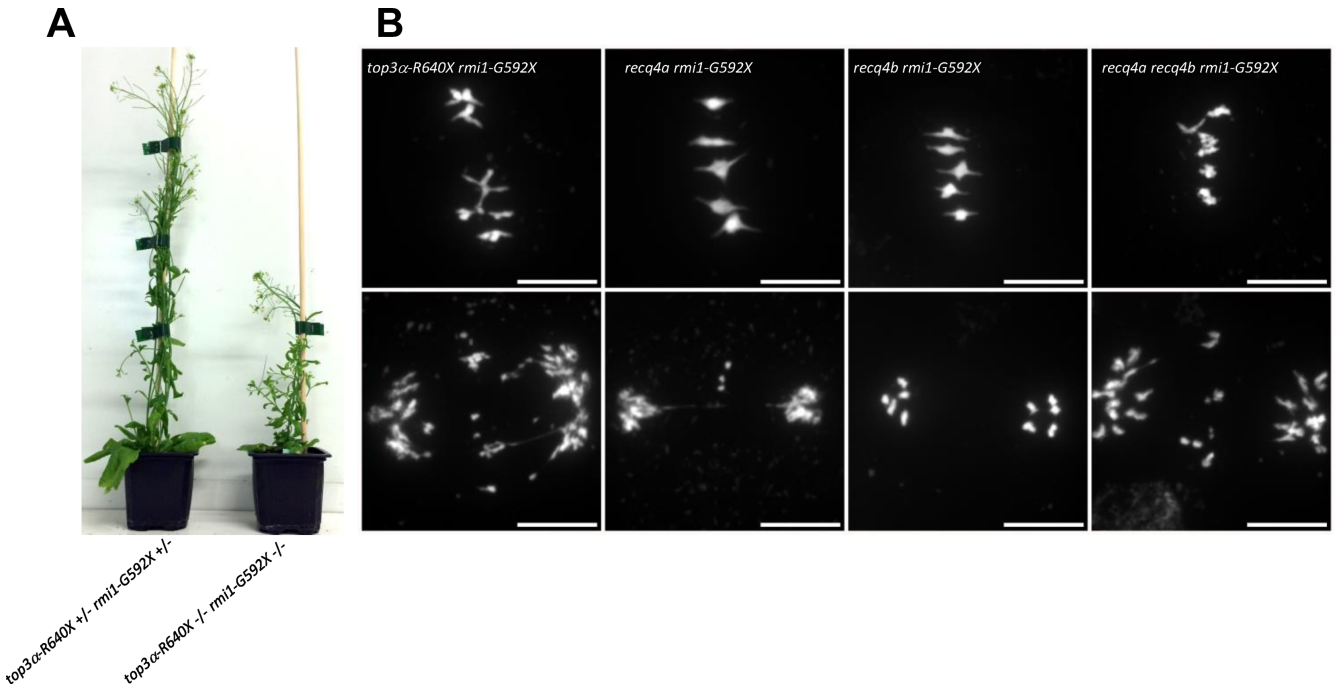

Figure 4. Genetic interactions between *rmi1-G592X*, *top3α-R640X* and *recq4ab* mutations. (**A**) Seven-week-old plants. The *top3α-R640X rmi1-G592X* double mutant shows a synthetic growth defect. (**B**) Chromosome spreads at metaphase I and anaphase I (scale bars, 10 μm).

rmi1-G592X mutation is at least partially non-redundant with the effect of the *fancm-1* mutation. Altogether, our results suggest that RMI1, like the other members of the BTR complex, TOP3α and RECQ4A/B, is a major anti-CO factor that limits class II CO formation in parallel to FANCM.

Genetic interactions between the different members of the BTR complex

Aiming to test if RMI1, TOP3α and RECQ4A/B limit COs together, we constructed the *rmi1-G592X top3α-R640X* double mutant and the *rmi1-G592X recq4a recq4b* triple mutant. As opposed to the *top3α-R640X* and *rmi1-G592X* single mutants, *top3α-R640X rmi1-G592X* displayed a somatic growth defect and was completely sterile (Figure 4A, Table 1). At meiosis, we observed abnormal bivalent structures at metaphase I, followed by chromatin bridges, massive chromosome fragmentation at anaphase I and meiotic arrest (Figure 4B). This result suggests that JM resolution is no longer proficient when *rmi1-G592X* and *top3α-R640X* are combined. Similarly, the *rmi1-G592X recq4a recq4b* triple mutant showed meiotic catastrophe whereas meiosis was normal in *rmi1-G592X recq4b* and only slightly affected in *rmi1-G592X recq4a* (Figure 4B). We previously described a similar meiotic catastrophe in the *top3α-R640X recq4a recq4b* triple mutant (16). In summary, meiotic catastrophe is observed in the three combinations *rmi1-G592X top3α-R640X, rmi1-G592X recq4a recq4b* and *top3α-R640X recq4a recq4b* (Table 1). This result suggests that even if the resolution of meiotic recombination intermediates is complete in *recq4ab*, or in *rmi1-G592X* or in *top3α-R640X*, unresolved recombination intermediates accumulate when two of these mutations are combined. Extra-COs in *recq4ab*, *top3α-R640X* (16) and *rmi-G592X* (Figure 1A) and chromosome fragmentation in *top3α-2* (15) and *rmi1-1* (14) are SPO11-1 dependent, but we cannot formerly exclude that meiotic catastrophe in multi-mutants arises from genomic instability rather than incomplete meiotic double strand breaks repair. The meiotic catastrophe prevent measurement of recombination in these genotypes and thus to directly test if RECQ4A/B, TOP3α and RMI1 act in the same anti-CO pathway. However, several arguments support this proposal: (i) They co-purify as a complex from somatic cells in *Arabidopsis* as in other species (16). (ii) The *rmi1-G592X* and the *recq4ab* mutations lead to a similar increase in CO frequency, which is higher than any other anti-CO mutant described so far (Figure 3B). (iii) the *recq4ab*, *top3α-R640X* and *rmi1-G592X* increase in CO is cumulative with *fancm* (16) (Figure 3B).

The oligo-binding fold domain 2 (OB2) of RMI1 is required to limit COs

Meiotic crossovers are increased by either disrupting *RECQ4A/B* or introducing particular alleles of either *TOP3α* or *RMI1* (Table 1). This raises the possibility that RMI1 and TOP3α have domains that are essential for anti-CO activity of the BTR complex but these same domains are not essential for preventing meiotic catastrophe.

In plants and human, RMI1 has three conserved domains. From N- to C-terminal: a domain of unknown function 1767 (DUF1767) and two oligonucleotide/oligosaccharide-binding fold domains (OB1 and OB2, Figure 2A and Supplementary Figure S1). Intriguingly, yeast Rmi1 is much shorter than the mammalian or plant counterparts and lacks the OB2 domain. Originally, OB fold domains were described as domains establishing protein-ssDNA interactions (reviewed

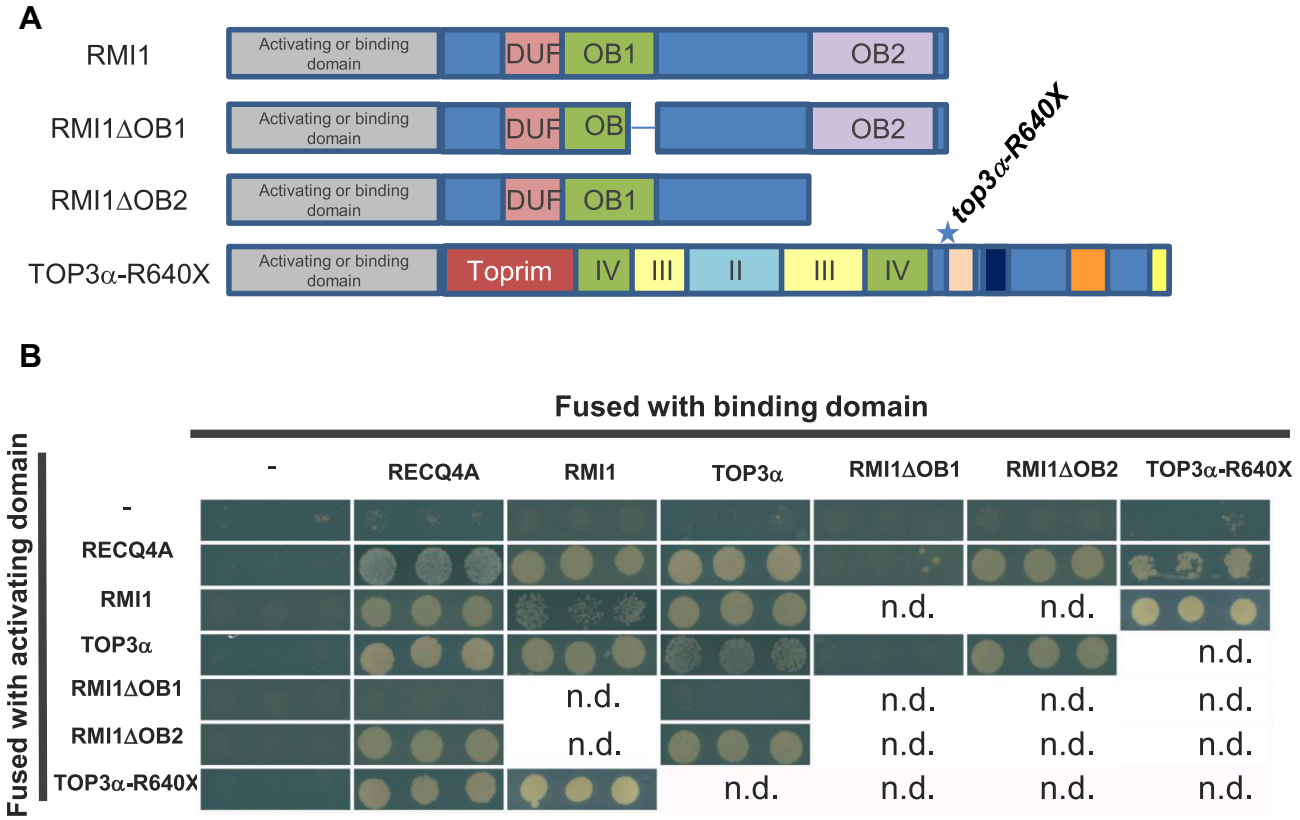

Figure 5. Deleting RMI1 OB2 fold domain and TOP3α Zn finger motifs does not alter protein–protein interactions between the different members of the BTR complex. (**A**) Schematic representation of the different fusion proteins used for the yeast two hybrid assays. (**B**) Yeast two-hybrid assays. Interaction between the bait fused with the GAL4 DNA binding domain (pGAD) and the pray fused with the GAL4 activation domain (pGBK) is revealed by growth on media depleted of histidine (-His). Three replicates are shown for each test. Untested combinations are indicated by n.d.

in (39)). Nevertheless, the OB1 domain of the human RMI1 protein does not possess DNA binding activity and was shown to mediate protein–protein interactions with TOP3α and BLM (40–42). Similarly, the human OB2 domain mediates an interaction with RMI2 which itself has an OB fold domain (also called OB3, (41)). In plants, as mentioned earlier, two studies described two *rmi1* mutants as completely sterile, showing aberrant bivalent structures at metaphase I, severe chromosome fragmentation at anaphase I and meiotic arrest before meiosis II (14,15). These two alleles (*rmi1-1* = *blap75-2* (15) and *blap75-1* (14)) are probably both null as they correspond to insertions within the open reading frame associated with deletions. The deletion in the *rmi1-1* allele spans from amino acid 91 to 408, i.e. lacking the DUF1767 and OB1 domains. In the *blap75-1* line, in addition to be disrupted, the *RMI1* ORF lacked its 5′ regions, including the DUF1767 domain. In addition, the meiotic function of the different domains was addressed by complementation experiment of *rmi1-1* mutants with full length or deleted versions of RMI1 protein (43). RMI1 proteins deleted of either the DUF1767 or the OB1 domain are unable to ensure the repair of meiotic recombination intermediates (43). The same study showed that an OB2-deleted version of *At*RMI1 restored meiotic progression with normal bivalent structures, complete repair of intermediates and fertility (43). Consistently, plants carrying the *rmi1-G592X* and *rmi1-G554R* mutations, both affecting the C-terminal OB2 domain of RMI1, were fertile and did not show chromosome fragmentation at anaphase I ($n = 47$ and $n = 10$ post anaphase I cells, respectively). This shows that the OB2 domain of RMI1 is dispensable for the repair of recombination intermediates and meiosis completion. In agreement with the dispensability of the OB2 domain for resolution of JMs *in planta*, the human RMI1 protein deleted of its OB2 domain remains active in dHJ dissolution *in vitro* (40,44). Nonetheless, the increase in crossovers that we detected in *rmi1-G592X* and *rmi1-G554R* mutants prompted us to propose that the OB2 domain is required to prevent extra-COs but is not essential for complete repair of recombination intermediates (at least in wild-type context for RECQ4 and TOP3α). Chelysheva *et al.*, had previously described several *rmi1* alleles that displayed neither sterility nor meiotic catastrophe, but these were not tested for an increase in CO formation (14). These alleles carry T-DNA insertions between the OB1 and OB2 domains (Salk_094387 = *rmi1-2*, Salk_054062 = *rmi1-4* and Salk_005449 = *rmi1-5*), and should display increased COs if the OB2 domain of RMI1 is essential for limiting CO formation. We introgressed the *msh5* mutation in these *rmi1* mutants and in an additional *rmi1* allele that also falls in between the OB domains (Salk_091373 = *rmi1-6*) and scored the number of bivalents at metaphase I. As in *msh5 rmi1-G592X*, the number of bivalents was higher in

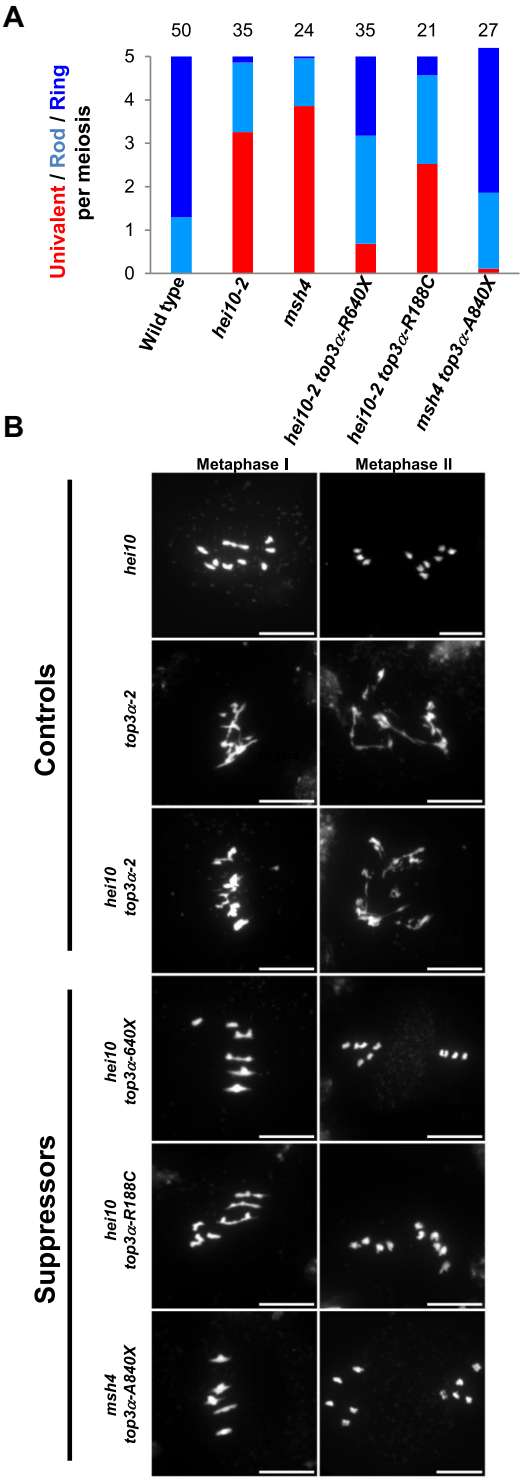

Figure 6. Separation of function mutations in TOP3α restore bivalent formation in *zmm* mutants. (**A**) Average number of bivalents per male meiocyte. Light blue bars represent rod bivalents, which have a rod shape with enlarged ends, indicating that one arm has at least one CO, whereas the other arm has no CO. Dark blue bars indicate ring bivalents, which have a lozenge shape, indicating that they have at least one CO on both arms. Red bars indicate pairs of univalents. The number of cells analyzed is indicated above each bar. (**B**) Chromosome spreads at metaphase I and metaphase II. (Scale bars, 10 μM). For *top3α-2* and *hei10 top3α-2*, images of anaphase I are displayed as meiosis does not proceed further in these genotypes.

msh5 rmi1-2, *msh5 rmi1-4, msh5 rmi1-5* and *msh5 rmi1-6* in comparison to the *msh5* single mutant (Figure 1A and B), showing that class II CO formation is increased by all of these mutations affecting the OB2 domain of RMI1. In addition, no fragmentation was observed at anaphase I (Figure 1B), meiosis could proceed beyond anaphase I and plants were fertile, showing that recombination intermediates are fully processed. This demonstrates that the RMI1 protein truncated of its OB2 fold domain is still able to ensure repair but not to prevent extra-COs. We explored the possibility that deleting the OB2 domain could affect the interaction between the members of the BTR complex, and showed in accordance with results obtained in mammals (40) that RMI1 interacts directly in yeast two hybrid assays with both RECQ4A and TOP3α through its OB1 domain and that OB2 is dispensable for these interactions (Figure 5).

The zinc finger domain of TOP3α is important to prevent CO formation

Animal and plant TOP3α contain several conserved domains including the Toprim domain (domain I), the Topoisomerase IA domain (domain II and III) and a C-terminal domain (domain V) containing one to five zinc fingers (Figure 2B and Supplementary Figure S1B) (44). Similar to *rmi1* mutations, mutations described in *TOP3α* in plants, affect differently its function (15,16). In addition, pursuing the *zmm* suppressor screen, we isolated a novel *top3α* allele mutated in the splice acceptor site of the last intron, leading to an altered coding sequence from Ala^{840}, hereafter named *top3α-A840X*. The *top3α-1* allele, which is likely null, is lethal (15). The *top3α-2* mutant, carrying a T-DNA insertion in an intron of the genic region encoding for the topoisomerase type IA domain (domain III, Figure 6B), is viable but shows somatic growth defects and meiotic catastrophe with massive chromosome entanglement and fragmentation, showing that TOP3α is essential for DNA repair at both mitosis and meiosis (15). In contrast, the *top3α-R640X* allele which encodes for a protein containing the Toprim and the topoisomerase domains but truncated of its C-terminal domain (V) has normal somatic growth, is able to fully resolve meiotic recombination intermediates, but shows increased CO formation (16). Similar to *top3α-R640X,* the *top3α-A840X* mutation affected neither the somatic function nor recombination intermediate resolution as assessed by normal growth and development and normal meiotic progression without chromosome fragmentation (Figure 6B). The *top3α-A840X* mutation restored CO formation in *zmm* mutants, more efficiently than the previously described *top3α-R640X* mutation (Figure 6A) (16). This shows that TOP3α possesses a meiotic anti-CO activity that can be uncoupled from its function ensuring full resolution of JMs. A dual function of Top3 has been established in yeast meiosis, where it both promotes NCO though early intermediate (D-loop) dissolution and is required to prevent meiotic catastrophe by disentangling late JMs (12,13,23). The *top3α-R640X* and *top3α-A840X* allele encodes for a protein truncated of the entire C-terminal domain (V) that contain four zinc finger motifs and for a protein truncated of the two last zinc fingers motifs, respectively. This shows

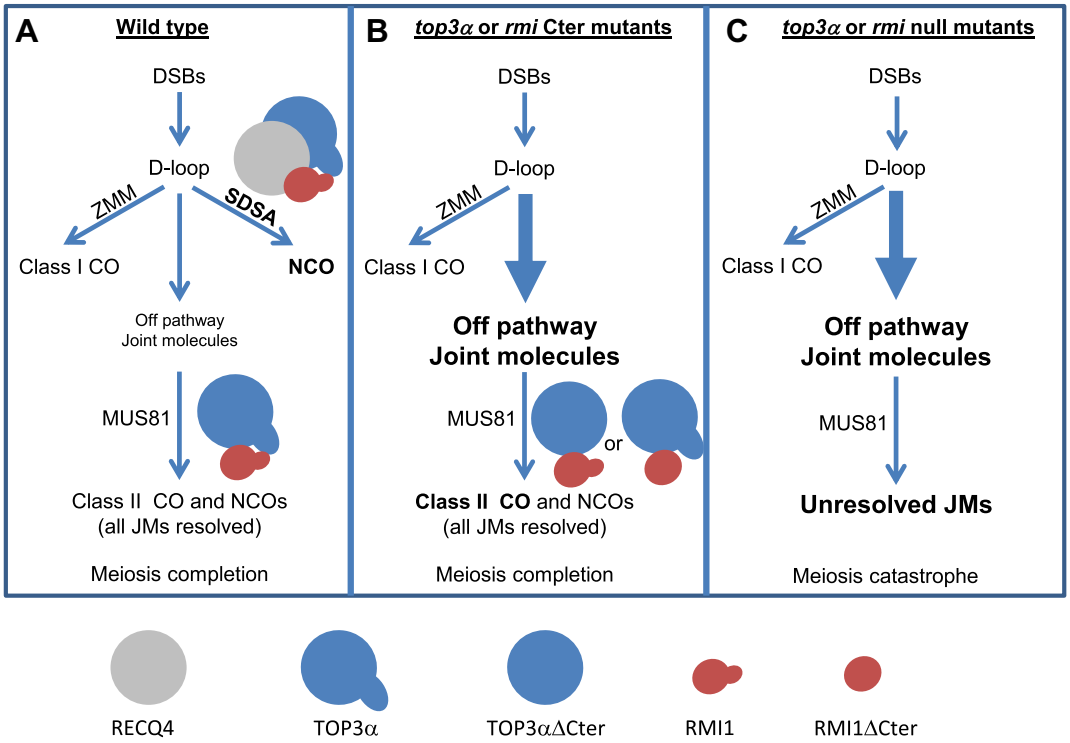

Figure 7. Proposed model of meiotic recombination, highlighting the specific role of RMI1 and TOP3α C-terminal domains in preventing extra-COs. (**A**) Schematic representation of DSB repair pathways in wild-type plants. After DSB formation, a large number of inter-homologous intermediates, also called D-loops, are formed. A subset of these intermediates is stabilized by ZMM proteins which promote Class I CO formation. The majority of D-loops is disassembled by the RECQ4-TOP3α-RMI1 pathway and is matured as Non-Crossovers (NCOs). A few events are neither processed by the class I nor SDSA pathways are referred to as 'off pathway joint molecules' (13). Part of these 'off pathway' events are resolved by MUS81 as class II COs. TOP3α and RMI1 play an essential role in removing remaining entanglements and promoting meiosis completion. (**B**) In the *top3α* and *rmi1* C-ter mutants, the TOP3αΔCter or RMI1ΔCter proteins are no longer proficient in disassembling D-loops with RECQ4, therefore a large number 'off pathway joint molecules' are formed. Part of these joint molecules are resolved by MUS81, leading to an increase in class II COs. The TOP3αΔCter and RMI1ΔCter proteins have kept their capacity to remove entanglements and to promote meiosis completion. (**C**) In absence of TOP3α and RMI1, not only a large amount of 'off pathway joint molecules' are formed but the machinery is unable to resolve the resulting rogue joint molecules. The presence of intertwined structures leads to chromosome bridges, fragmentation and meiotic arrest.

that the domain V of AtTOP3α, and notably the zinc finger motifs, are dispensable for the full resolution of JMs but required to prevent extra-CO formation. We showed that the domain V is dispensable for the interaction of TOP3α with RECQ4A and RMI1 in yeast two hybrid assays (Figure 5B). This is in accordance with the ability of truncated human TOP3α, lacking the domain V, to promote dHJ dissolution *in vitro* (44). In contrast, this C-terminal domain V is crucial to prevent extra-CO formation at meiosis in *Arabidopsis*. We suggest that the meiotic anti-CO activity of TOP3α does not rely on dHJ or related intermediates dissolution activity, but rather on its capacity to reverse D-loops (23). Interestingly, we isolated a third *top3α* allele that was able to partially restore CO formation in *hei10* (Figure 6A) without showing any chromosome fragmentation at meiosis (Figure 6B). In contrast to *top3α-R640X* and *top3α-A840X* mutations, this mutation did not affect the C-terminal domain of TOP3α but consisted of an amino acid change Arg^{188} to Cys, named hereafter *top3α-R188C* (Figure 2B). According to the human TOP3α crystal structure (44), this amino acid belongs to the non-catalytic CAP domain IV which in the 3D structure is located in close vicinity of the C-terminal part of the TOP3α protein. This suggests that the non-catalytic CAP domain IV together with the zinc-finger containing domain V of TOP3α could form a structural domain that is required to limit CO formation but not to remove hemicatenates or relieve topological constrains.

On an applied perspective, our results suggest that specific mutations of *RMI1* and *TOP3α* could be used to increase recombination and thus facilitating breeding in crops. It would be notably particularly interesting to test if manipulating the BTR complex could unlock CO formation (and therefore genetic diversity) in CO-poor regions such as the large pericentromeric regions in cereals (45).

Multiple functions of BTR at meiosis

RMI-1 and HIM-6 (BLM) have been also shown to facilitate class I CO in *C. elegans* (46,47). Intriguingly, *Arabidopsis rmi1-4*, *rmi1-5* and *top3α-R640X* single mutants show some univalents at metaphase I (about 1 for every 8 cells, Figure 1A and (16)), while they largely restore CO in *zmms*. This subtle defect of the single mutant suggests that the obligate crossover is not fully implemented, and thus that a small subset of class I COs are not formed in these backgrounds, in accordance with the pro-CO role of RMI1 described in *C.elegans.* It is possible that this slight defect in class I CO could be compensated in the *Arabidopsis rmi1-*

G592X, rmi1-2, rmi-6 or *recq4ab* mutants, by a larger increase in class II CO formation that make it unlikely for a pair of homologues not to receive at least one CO. This is supported by their greater effect in restoring CO in *zmm* mutants than *rmi1-4*, *rmi1-5* and *top3α-R640X*.

Data obtained in yeast, *C. elegans* and *Arabidopsis* converge to the conclusion that the BTR complex plays multiple functions in meiotic recombination, with: (i) the three subunits being required to promote NCO/prevent unregulated CO formation through D-loop dissolution; (ii) TOP3α, RMI1 but not the BLM homologs being required to dissolve late recombination intermediates or preventing the formation of unresolvable intermediates, thus ensuring meiosis completion. Two possibilities may explain why the BLM homolog is not essential for this function. First, some repair intermediates may contain single-strand DNA that can be decatenate by TOP3α-RMI1. Alternatively, other helicases such as other RECQ homologues may provide ssDNA to TOP3α-RMI1 and (iii) the BTR complex possibly promoting the maturation of a subset of class I CO (13,14,16,17,24,25,37 and this study).

In addition, we show here that the C-terminal domains of RMI1 and TOP3α, which contain an OB fold and zing finger motifs respectively, are essential to prevent extra-CO formation, but not required to ensure chromosome integrity at meiosis. One possibility is that the truncation of the C-terminal domain of TOP3α or RMI1 decreases the topoisomerase activity of the complex below a higher threshold needed to repress class II crossovers, while maintaining a level of activity above a threshold needed for viability and for intermediate resolution. The defect in repair observed when combining two of the *recq4ab*, *top3α-R640X* or *rmi1-G592X* mutations (Figure 4) favors this first possibility. However, a dual function of the Top3-Rmi1 complex has been reported in yeast meiosis (12,13): (i) at early meiosis, together with Sgs1, Top3-Rmi1 promote NCO formation via D-loop displacement; (ii) at a later stage Top3-Rmi1 ensure full resolution of recombination intermediates. Therefore, we propose an alternative model in which the two functions of TOP3α-RMI1 in preventing COs and ensuring chromosome disentanglements rely on distinct biochemical activities. In this model, (Figure 7) the C-terminal domains of RMI1 and TOP3α form a structure, which is crucial for dissolution of early recombination intermediates by the BTR complex, possibly by direct recognition of D-loops by the OB fold and/or the zinc finger motifs. Supporting this idea, the zinc fingers of the *Drosophila* TOP3α have been shown to be major contributors to DNA binding (48). The RMI1 and TOP3α C-terminal domains may also facilitate the repair function of these proteins, but in a dispensable manner as the lack of these domains leads to repair defects only if other members of the complex are concomitantly mutated. The crystal structures of co-crystalized human RMI1 and TOP3α described so far lack precisely these C-terminal domains. Our results suggests future direction in the study of the BTR complex, notably in describing the structure of full length proteins and comparing the dissolution activity of the BTR complex with or without the C-terminal domains of TOP3α and RMI1 on DNA structures, notably D-loops.

SUPPLEMENTARY DATA

Supplementary Data are available at NAR Online.

ACKNOWLEDGEMENTS

We wish to thank Mathilde Grelon, Christine Mezard, Eric Jenczewski, Rajeev Kumar and Charlotte Hodson for critical reading of the manuscript. We wish to thank Gregory Copenhaver for providing the FTL lines.

FUNDING

European Research Council (ERC) [2011 StG 281659, MeioSight]; Fondation Simone et Cino del Duca and the Fondation Schlumberger pour l'Enseignement et la Recherche; Labex Saclay Plant Sciences (SPS) [ANR-10-LABX-0040-SPS to I.J.P.B.]. Funding for open access charge: ERC [2011 StG 281659, MeioSight].
Conflict of interest statement. None declared.

REFERENCES

1. Hunter,N. (2015) Meiotic Recombination: The Essence of Heredity. *Cold Spring Harb. Perspect. Biol.*, **7**, 1–35.
2. Lynn,A., Soucek,R. and Börner,G.V. (2007) ZMM proteins during meiosis: crossover artists at work. *Chromosome Res.*, **15**, 591–605.
3. Mercier,R., Mezard,C., Jenczewski,E., Macaisne,N. and Grelon,M. (2015) The molecular biology of meiosis in plants. *Annu. Rev. Plant Biol.*, **66**, 297–327.
4. Börner,G.V., Kleckner,N. and Hunter,N. (2004) Crossover/noncrossover differentiation, synaptonemal complex formation, and regulatory surveillance at the leptotene/zygotene transition of meiosis. *Cell*, **117**, 29–45.
5. Zakharyevich,K., Tang,S., Ma,Y. and Hunter,N. (2012) Delineation of joint molecule resolution pathways in meiosis identifies a crossover-specific resolvase. *Cell*, **149**, 334–347.
6. Berchowitz,L.E., Francis,K.E., Bey,A.L. and Copenhaver,G.P. (2007) The role of AtMUS81 in interference-insensitive crossovers in A. thaliana. *PLoS Genet.*, **3**, e132.
7. de Los Santos,T, Hunter,N., Lee,C., Larkin,B., Loidl,J. and Hollingsworth,N.M. (2003) The Mus81/Mms4 endonuclease acts independently of double-Holliday junction resolution to promote a distinct subset of crossovers during meiosis in budding yeast. *Genetics*, **164**, 81.
8. Holloway,J.K., Booth,J., Edelmann,W., McGowan,C.H. and Cohen,P.E. (2008) MUS81 generates a subset of MLH1-MLH3-independent crossovers in mammalian meiosis. *PLoS Genet.*, **4**, e1000186.
9. Chelysheva,L., Vezon,D., Chambon,A., Gendrot,G., Pereira,L., Lemhemdi,A., Vrielynck,N., Le Guin,S., Novatchkova,M. and Grelon,M. (2012) The *Arabidopsis* HEI10 is a new ZMM protein related to Zip3. *PLoS Genet.*, **8**, e1002799.
10. Cole,F., Kauppi,L., Lange,J., Roig,I., Wang,R., Keeney,S. and Jasin,M. (2012) Homeostatic control of recombination is implemented progressively in mouse meiosis. *Nat. Cell Biol.*, **14**, 424–430.
11. De Muyt,A., Jessop,L., Kolar,E., Sourirajan,A., Chen,J., Dayani,Y. and Lichten,M. (2012) BLM helicase ortholog Sgs1 Is a central regulator of meiotic recombination intermediate metabolism. *Mol. Cell*, **46**, 43–53.
12. Kaur,H., De Muyt,A. and Lichten,M. (2015) Top3-Rmi1 DNA single-strand decatenase is integral to the formation and resolution of meiotic recombination intermediates. *Mol. Cell*, **57**, 583–594.
13. Tang,S., Wu,M.K.Y., Zhang,R. and Hunter,N. (2015) Pervasive and essential roles of the Top3-Rmi1 decatenase orchestrate recombination and facilitate chromosome segregation in meiosis. *Mol. Cell*, **57**, 607–621.
14. Chelysheva,L., Vezon,D., Belcram,K., Gendrot,G. and Grelon,M. (2008) The *Arabidopsis* BLAP75/Rmi1 homologue plays crucial roles in meiotic double-strand break repair. *PLoS Genet.*, **4**, e1000309.

15. Hartung,F., Suer,S., Knoll,A., Wurz-Wildersinn,R. and Puchta,H. (2008) Topoisomerase 3alpha and RMI1 suppress somatic crossovers and are essential for resolution of meiotic recombination intermediates in *Arabidopsis thaliana*. *PLoS Genet.*, **4**, e1000285.
16. Séguéla-Arnaud,M., Crismani,W., Larchevêque,C., Mazel,J., Froger,N., Choinard,S., Lemhemdi,A., Macaisne,N., Van Leene,J., Gevaert,K. *et al.* (2015) Multiple mechanisms limit meiotic crossovers: TOP3α and two BLM homologs antagonize crossovers in parallel to FANCM. *Proc. Natl. Acad. Sci. U.S.A.*, **112**, 4713–4718.
17. Wu,L. and Hickson,I.D. (2003) The Bloom's syndrome helicase suppresses crossing over during homologous recombination. *Nature*, **426**, 870–874.
18. Wu,L., Bachrati,C.Z., Ou,J., Xu,C., Yin,J., Chang,M., Wang,W., Li,L., Brown,G.W. and Hickson,I.D. (2006) BLAP75/RMI1 promotes the BLM-dependent dissolution of homologous recombination intermediates. *Proc. Natl. Acad. Sci. U.S.A.*, **103**, 4068–4073.
19. Bussen,W., Raynard,S., Busygina,V., Singh,A.K. and Sung,P. (2007) Holliday junction processing activity of the BLM-Topo IIIalpha-BLAP75 complex. *J. Biol. Chem.*, **282**, 31484–31492.
20. Cejka,P., Plank,J.L., Bachrati,C.Z., Hickson,I.D. and Kowalczykowski,S.C. (2010) Rmi1 stimulates decatenation of double Holliday junctions during dissolution by Sgs1-Top3. *Nat. Struct. Mol. Biol.*, **17**, 1377–1382.
21. van Brabant,a J., Ye,T., Sanz,M., German,J.L. III, Ellis,N.A. and Holloman,W.K. (2000) Binding and melting of D-loops by the Bloom syndrome helicase. *Biochemistry*, **39**, 14617–14625.
22. Bachrati,C.Z., Borts,R.H. and Hickson,I.D. (2006) Mobile D-loops are a preferred substrate for the Bloom's syndrome helicase. *Nucleic Acids Res.*, **34**, 2269–2279.
23. Fasching,C.L., Cejka,P., Kowalczykowski,S.C. and Heyer,W.-D. (2015) Top3-Rmi1 dissolve Rad51-mediated D loops by a topoisomerase-based mechanism. *Mol. Cell*, **57**, 595–606.
24. Hartung,F., Suer,S. and Puchta,H. (2007) Two closely related RecQ helicases have antagonistic roles in homologous recombination and DNA repair in *Arabidopsis thaliana*. *Proc. Natl. Acad. Sci. U.S.A.*, **104**, 18836–18841.
25. Crismani,W., Girard,C., Froger,N., Pradillo,M., Santos,J.L., Chelysheva,L., Copenhaver,G.P., Horlow,C. and Mercier,R. (2012) FANCM limits meiotic crossovers. *Science*, **336**, 1588–1590.
26. Drouaud,J., Khademian,H., Giraut,L., Zanni,V., Bellalou,S., Henderson,I.R., Falque,M. and Mezard,C. (2013) Contrasted patterns of crossover and non-crossover at *Arabidopsis thaliana* meiotic recombination hotspots. *PLoS Genet.*, **9**, e1003922.
27. Higgins,J.D., Vignard,J., Mercier,R., Pugh,A.G., Franklin,F.C.H. and Jones,G.H. (2008) AtMSH5 partners AtMSH4 in the class I meiotic crossover pathway in *Arabidopsis thaliana*, but is not required for synapsis. *Plant J.*, **55**, 28–39.
28. Macaisne,N., Novatchkova,M., Peirera,L., Vezon,D., Jolivet,S., Froger,N., Chelysheva,L., Grelon,M. and Mercier,R. (2008) SHOC1, an XPF endonuclease-related protein, is essential for the formation of class I meiotic crossovers. *Curr. Biol.*, **18**, 1432–1437.
29. Berchowitz,L.E. and Copenhaver,G.P. (2008) Fluorescent *Arabidopsis* tetrads: a visual assay for quickly developing large crossover and crossover interference data sets. *Nat. Protoc.*, **3**, 41–50.
30. Girard,C., Crismani,W., Froger,N., Mazel,J., Lemhemdi,A., Horlow,C. and Mercier,R. (2014) FANCM-associated proteins MHF1 and MHF2, but not the other Fanconi anemia factors, limit meiotic crossovers. *Nucleic Acids Res.*, **42**, 9087–9095.
31. Ross,K.J., Fransz,P. and Jones,G.H. (1996) A light microscopic atlas of meiosis in *Arabidopsis thaliana*. *Chromosom. Res.*, **4**, 507–516.
32. Chelysheva,L., Grandont,L., Vrielynck,N., le Guin,S., Mercier,R. and Grelon,M. (2010) An easy protocol for studying chromatin and recombination protein dynamics during *Arabidopsis thaliana* meiosis: immunodetection of cohesins, histones and MLH1. *Cytogenet. Genome Res.*, **129**, 143–153.
33. Perkins,D.D. (1949) Biochemical Mutants in the Smut Fungus Ustilago Maydis. *Genetics*, **34**, 607–626.
34. Scott,S.P., Teh,A., Peng,C. and Lavin,M.F. (2002) One-step site-directed mutagenesis of ATM cDNA in large (20kb) plasmid constructs. *Hum. Mutat.*, **20**, 323.
35. Girard,C., Chelysheva,L., Choinard,S., Froger,N., Macaisne,N., Lemhemdi,A., Lehmemdi,A., Mazel,J., Crismani,W. and Mercier,R. (2015) AAA-ATPase FIDGETIN-LIKE 1 and helicase FANCM antagonize meiotic crossovers by distinct mechanisms. *PLoS Genet.*, **11**, e1005369.
36. Hartung,F., Suer,S., Bergmann,T. and Puchta,H. (2006) The role of AtMUS81 in DNA repair and its genetic interaction with the helicase AtRecQ4A. *Nucleic Acids Res.*, **34**, 4438–4448.
37. Bellaoui,M., Chang,M., Ou,J., Xu,H., Boone,C. and Brown,G.W. (2003) Elg1 forms an alternative RFC complex important for DNA replication and genome integrity. *EMBO J.*, **22**, 4304–4313.
38. Tong,A.H.Y., Lesage,G., Bader,G.D., Ding,H., Xu,H., Xin,X., Young,J., Berriz,G.F., Brost,R.L., Chang,M. *et al.* (2004) Global mapping of the yeast genetic interaction network. *Science*, **303**, 808–813.
39. Flynn,R.L. and Zou,L. (2010) Growing family of genome guardians. *Crit. Rev. Biochem. Mol. Biol.*, **45**, 266–275.
40. Raynard,S., Zhao,W., Bussen,W., Lu,L., Ding,Y.-Y., Busygina,V., Meetei,A.R. and Sung,P. (2008) Functional role of BLAP75 in BLM-topoisomerase IIIalpha-dependent holliday junction processing. *J. Biol. Chem.*, **283**, 15701–15708.
41. Wang,F., Yang,Y., Singh,T.R., Busygina,V., Guo,R., Wan,K., Wang,W., Sung,P., Meetei,A.R. and Lei,M. (2010) Crystal structures of RMI1 and RMI2, two OB-fold regulatory subunits of the BLM complex. *Structure*, **18**, 1159–1170.
42. Xu,D., Guo,R., Sobeck,A., Bachrati,C.Z., Yang,J., Enomoto,T., Brown,G.W., Hoatlin,M.E., Hickson,I.D. and Wang,W. (2008) RMI, a new OB-fold complex essential for Bloom syndrome protein to maintain genome stability. *Genes Dev.*, **22**, 2843–2855.
43. Bonnet,S., Knoll,A., Hartung,F. and Puchta,H. (2013) Different functions for the domains of the *Arabidopsis thaliana* RMI1 protein in DNA cross-link repair, somatic and meiotic recombination. *Nucleic Acids Res.***41**, 9349–9360.
44. Bocquet,N., Bizard,A.H., Abdulrahman,W., Larsen,N.B., Faty,M., Cavadini,S., Bunker,R.D., Kowalczykowski,S.C., Cejka,P., Hickson,I.D. *et al.* (2014) Structural and mechanistic insight into Holliday-junction dissolution by topoisomerase IIIα and RMI1. *Nat. Struct. Mol. Biol.*, **21**, 261–268.
45. Choulet,F., Alberti,A., Theil,S., Glover,N., Barbe,V., Daron,J., Pingault,L., Sourdille,P., Couloux,A., Paux,E. *et al.* (2014) Structural and functional partitioning of bread wheat chromosome 3B. *Science*, **345**, 1249721.
46. Jagut,M., Hamminger,P., Woglar,A., Millonigg,S., Paulin,L., Mikl,M., Dello Stritto,M.R., Tang,L., Habacher,C., Tam,A. *et al.* (2016) Separable roles for a Caenorhabditis elegans RMI1 homolog in promoting and antagonizing meiotic crossovers ensure faithful chromosome inheritance. *PLoS Biol.*, **14**, e1002412.
47. Schvarzstein,M., Pattabiraman,D., Libuda,D.E., Ramadugu,A., Tam,A., Martinez-Perez,E., Roelens,B., Zawadzki,K.A., Yokoo,R., Rosu,S. *et al.* (2014) DNA helicase HIM-6/BLM both promotes MutSγ-dependent crossovers and antagonizes MutSγ-independent inter-homolog associations during Caenorhabditis elegans meiosis. *Genetics*, doi:10.1534/genetics.114.161513.
48. Chen,S.H., Wu,C.H., Plank,J.L. and Hsieh,T.S. (2012) Essential functions of C terminus of Drosophila topoisomerase IIIα in double holliday junction dissolution. *J. Biol. Chem.*, **287**, 19346–19353.